

AI-based control techniques for maximum power point tracking of photovoltaic systems using a boost converter

Abstract. This paper proposes an artificial intelligence (AI)-based control approach for maximum power point tracking (MPPT) of photovoltaic (PV) systems using a boost converter. The proposed method utilizes an artificial neural network (ANN) and Adaptive Neuro-Fuzzy Inference Systems (ANFIS) to predict the optimal duty cycle for the boost converter. Both approaches are trained using a dataset obtained through MATLAB simulations under various operating conditions. The paper also includes a comparison of the proposed AI algorithm with the classical MPPT algorithm.

Streszczenie. W artykule zaproponowano podejście oparte na sztucznej inteligencji (AI) do śledzenia punktu maksymalnej mocy (MPPT) systemów fotowoltaicznych (PV) z wykorzystaniem przetwornicy podwyższającej napięcie. Proponowana metoda wykorzystuje sztuczną sieć neuronową (ANN) i adaptacyjne systemy wnioskowania neurorozmytego (ANFIS) do przewidywania optymalnego cyklu pracy przetwornicy podwyższającej napięcie. Oba podejścia są szkolone przy użyciu zbioru danych uzyskanego w drodze symulacji w różnych warunkach operacyjnych. Artykuł zawiera również porównanie proponowanego algorytmu AI z klasycznym algorytmem MPPT. (Techniki sterowania oparte na sztucznej inteligencji do śledzenia punktu maksymalnej mocy systemów fotowoltaicznych za pomocą przetwornicy podwyższającej napięcie)

Keywords: Artificial Intelligence, MPPT, Photovoltaic, DC-DC converter

Słowa kluczowe: Sztuczna inteligencja, MPPT, fotowoltaika, przetwornica DC-DC

Introduction

The utilization of PV systems as a reliable and sustainable source of energy has been on the rise due to their many advantages, including their eco-friendliness, ready availability, and cost-effectiveness. Furthermore, these systems operate silently and require minimal maintenance. PV systems use solar panels to convert sunlight into electricity [1], which can then be used to power homes and businesses. As PV system is typically non-linear in terms of the characteristic power curve, which changes with temperature and irradiance [2, 3], it is suffering from a low-efficiency problem. Consequently, PV systems must effectively track their maximum power at each level of irradiance and panel temperature to maximize energy conversion efficiency. To achieve this, many MPPT techniques, including Perturb and Observe (P&O), Incremental Conductance (IC), Sliding Mode Control (SMC) [4] have been developed and compared over the years. However, these classical MPPT algorithms have certain drawbacks, such as poor tracking accuracy, low convergence speed, and sensitivity to varying weather conditions.

This paper proposes an AI-based MPPT technique for PV systems using ANN and ANFIS to overcome the problem of the Classical MPPT algorithm. The proposed MPPT algorithm predicts the optimal duty cycle of the boost converter, which can be used to match the load and source impedance to maximize the energy transfer between the PV panel and the load. The effectiveness of the proposed algorithm was tested through simulation results under different variation levels of irradiance and temperature.

ANN-based MPPT algorithm

To address the limitations of the classical MPPT algorithm, advanced techniques such as ANN have been developed, as evidenced by studies [5, 6, 7, 8] and accompanied by the advancement of Fuzzy Logic Controller

(FLC) technology [9, 10, 11, 12, 13]. As indicated in fig. 1, the ANN approach comprises three layers - input, hidden layer, and output, wherein for solar MPPT applications, inputs are temperature and irradiance while tracked maximum voltage serves as the output. The converter duty cycle is controlled by the difference between tracked voltage and PV voltage. The performance of ANN depends on the structure of its hidden layer, with a greater number of neurons resulting in superior tracking performance. The general work flowchart of ANN-based MPPT algorithm is depicted in fig. 2.

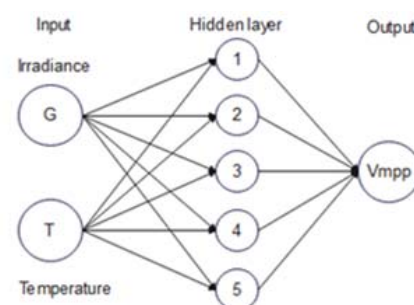


Fig.1. ANN structure

ANFIS-based MPPT algorithm

ANFIS is a combination of ANN and FLC, which is used for pattern recognition, classification, and regression tasks, and are adaptive, meaning they learn from data to improve accuracy. ANFIS models consist of five layers, each of which performs a specific function in the inference process. The first layer takes the input variables and applies membership functions to fuzzify the input data. The second layer calculates the degree of membership of each input variable to each of the fuzzy sets. The third layer applies fuzzy logic to make decisions about the system's output based on the input variables and their membership

functions. The fourth layer calculates the weighted averages of the outputs from the third layer. The fifth and final layer provides the over-all output of the ANFIS model. ANFIS is well-suited to problems with complex, non-linear relationships between inputs and outputs and has been used in various applications, including control systems for solar MPPT. The work flowchart is depicted in fig. 3.

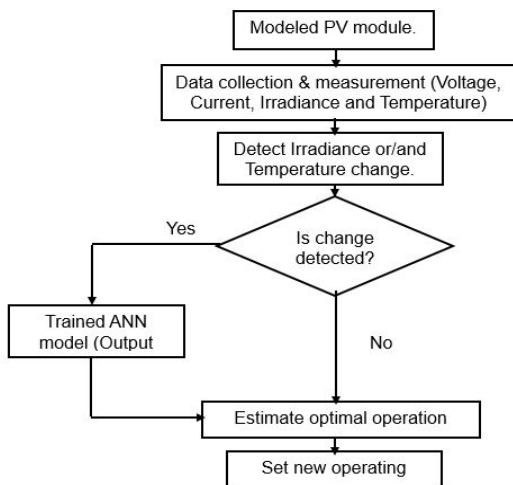


Fig.2. Work flowchart for ANN-based MPPT algorithm

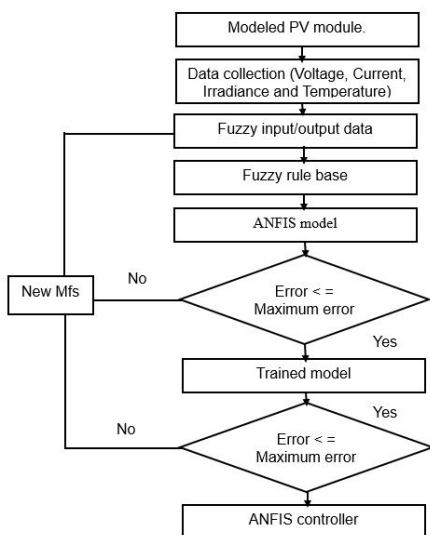


Fig.3. Work flowchart for ANFIS-based MPPT algorithm

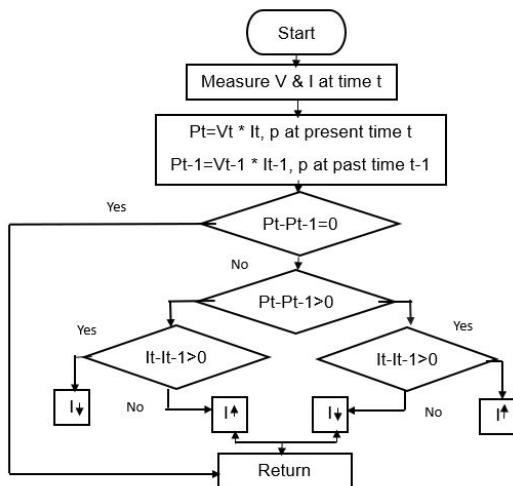


Fig.4. Work flowchart for P&O - based MPPT algorithm

P & O-based MPPT algorithm

P&O is a popular MPPT method, easy to use and implement [14], either through direct duty ratio or voltage reference control, and comparing the past and present values at time t & $(t-1)$. It measures PV array voltage and current and then calculates power. P&O algorithm work flowchart is indicated in fig. 4. Despite its ease, simplicity, and ability to be applied to any type of solar panel, the P&O method has its drawbacks in tracking time and oscillation around the maximum power point (MPP) [15], especially, under rapid environmental changes.

Methodology

As depicted in fig. 5, the main elements of optimized PV system design are PV module, boost converter, and intelligent MPPT algorithms. To achieve maximum power tracking, the PV system's modelling methodology involves three essential steps: data collection of irradiances, temperature, voltage, and current; boost converter design; and training of the proposed AI-based MPPT algorithms.

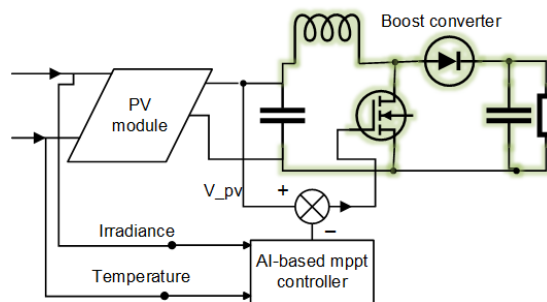


Fig.5. Block diagram of PV system with intelligent control algorithm

Data collection

A large amount of data, including current and voltage measurements, was collected from multiple irradiance and temperature levels. The effect of irradiance and temperature to the output current of the PV panel is determined from the equivalent circuit, as illustrated in fig. 6, which comprises electrical parameters such as a photocurrent source (I_{ph}), a diode (D), a series resistor (R_s), and a shunt resistor (R_{sh}) [16, 17]. The value of I_{ph} is dependent on the irradiance or insolation that reaches the solar cell. This irradiance generates a fixed amount of photocurrent. As the irradiance changes, the photocurrent source also varies accordingly.

Table 1. Electrical specifications of 230 Wp PV module

Parameter	Value
Maximum power (P_{MPP})	230 Wp
Cells per module (Ncell)	60
Open circuit voltage (VOC) (V)	36.2
Short-circuit current (Isc) (A)	8.1
Voltage at maximum power point (Vmp) (V)	30.36
Current at maximum power point (Imp) (A)	7.58
Temperature coefficient of VOC (β , %/deg.C)	-0.359
Temperature coefficient of Isc (α , %/deg.C)	0.097

Kirchhoff's law applied to the equivalent circuit in fig. 6, yields the PV output current (I_{out}), which is practically expressed by (1) and (2).

$$(1) \quad I_{out} = I_{ph} - I_d - I_{sh}$$

$$(2) \quad I_{out} = I_{ph} - I_o \left(e^{\frac{q(V+IR_s)}{aKT_c}} - 1 \right) - \frac{V+IR_s}{R_{sh}}$$

where: I_o - inverse saturation current of the diode, I_{sh} - shunt resistor current, I_d - diode current, q - charge of an electron, V - solar cell voltage, K - Boltzmann constant, T_c - operating temperature, a – identity factor.

$$(3) \quad I_{ph} = \frac{G}{G_{ref}} \left[I_{ref} + a I_{sc} (T_c - T_{cref}) \right]$$

$$(4) \quad I_o = I_{oref} \left(\frac{T_c}{T_{cref}} \right)^3 e^{\left[\frac{qE_G}{aK} \left(\frac{1}{T_{cref}} - \frac{1}{T_c} \right) \right]}$$

where: G - irradiance collected by solar cell, G_{ref} irradiance at standard conditions (1 kW/m^2), I_{ref} generated photocurrent at reference conditions, $a I_{sc}$ - short-circuit current temperature coefficient, T_{cref} (298 K) - operating temperature at standard condition.

$$(5) \quad I_{oref} = \frac{I_{sc}}{\left(\frac{q(V_{oc})}{N_s a K T_c} - 1 \right)}$$

where: I_{sc} - short-circuit current, I_{oref} inverse saturation current at reference conditions, V_{oc} - open-circuit voltage.

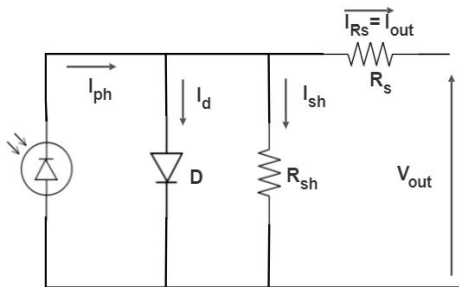


Fig.6. PV equivalent circuit

To create a PV module that generates the desired power, solar cells must be connected in series or parallel. For this case, the number of parallel modules (N_p) and the number of solar cells (N_s) are added to equation (5) as coefficients of solar cells, and this represents the current-voltage characteristic of the PV panel, as shown in (6).

$$(6) \quad I_{out} = N_s I_{ph} - N_p I_o \left(e^{\left(\frac{q(V - I R_s)}{N_s a K T_c} \right)} - 1 \right) - \frac{V - I R_s}{R_{sh}}$$

The PV characteristics curve of the proposed PV panel, along with its electrical specifications as outlined in table. 1, are depicted in fig. 7 and fig. 8, under various irradiance and temperature levels.

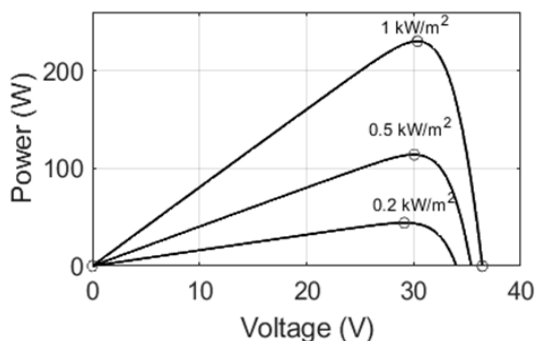


Fig.7. PV characteristics curve for variable irradiance at constant temperature ($25 \text{ }^\circ\text{C}$)

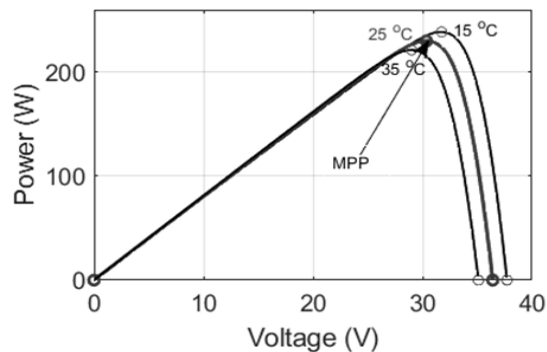


Fig.8. PV characteristics curve for variable Temperature at constant Irradiance (1 kW/m^2)

Design of DC - DC (boost) converter

The DC - DC converter serves as an interface between the load and the PV module, transferring maximum power from the solar PV module to the load. Its operation depends on the activation signal of the power switch converter (IGBT), as shown in fig. 9. In this paper, the IGBT's state is controlled by AI-based MPPT controllers. The boost converter operates in two modes of operation, depending on the IGBT's state. In the first mode, when the switch is closed, it operates as a short circuit with ideally zero resistance, allowing current to flow through it and back to the input source. The diode becomes an open circuit, limiting current flow to the load, as a result the load requirement met from the capacitor. In the second mode, the switch is open, and the energy stored in the inductor is released and dissipated in the load resistance. The diode is on its conducting mode, and the source charges the capacitor and satisfies the load needs. The IGBT is selected as the power switch converter for the proposed boost converter due to its higher voltage and current rating than the input.

The internal resistance and snubber resistance of the IGBT are chosen as $1000 \text{ m}\Omega$ and 105Ω respectively. For the diode, a forward-biased diode is selected with a resistance of 0.001Ω and snubber resistance of 500Ω . The parameters of the boost converter are calculated based on electrical specification of the PV panel, load requirement, switching frequency (f_s): 25 kHz , Voltage ripple factor 0.5 and current ripple factor is chosen as 40% (ripple current factor is according to IEC standard). The calculation for all parameter is shown in (7) to (13).

$$(7) \quad \text{Duty cycle} = \frac{(V_{out} - V_{in})}{V_{out}}$$

$$(8) \quad I_{out} = \frac{P_{MPP}}{V_{out}}$$

$$(9) \quad \Delta V = V_{out} * V_{ripple}$$

$$(10) \quad \Delta I = I_{out} * I_{ripple}$$

$$(11) \quad R = \frac{V_{out}}{I_{out}}$$

$$(12) \quad C = \frac{I_{out} * D}{f_s * \Delta V} = C_1 = C_2$$

$$(13) \quad L = \frac{V_{out} * (V_{out} - V_{in})}{V_{out} * f_s * \Delta I}$$

Where: C_1 & C_2 are input & output capacitors respectively, R is load resistance, and L is an inductor.

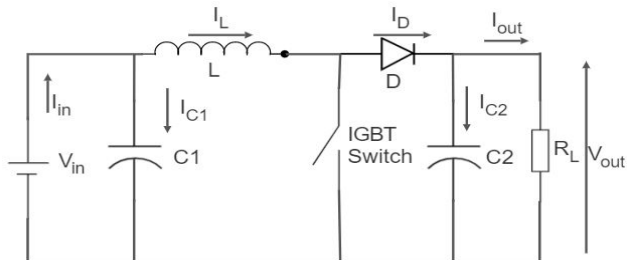


Fig.9. DC – DC (boost) converter

Table 2. Boost converter specification

Parameter	Value
R_L	15.6434 Ω
C_1	2.6557e-04 F
C_2	2.6557e-04 F
L	1.9786e-04 H
f_s	25 kHz

ANN training, test, and performance evaluation

ANN is a parallel and distributed data processing system, that comprises substantial number of neurons and features including an architecture, activation function, and training method. Neurons are linked and guided by related weights to construct the ANN. In this study, the ANN is trained using two inputs (irradiance and temperature) and one output (V_{MPP}). The feed forward neural network with 20 hidden layer neurons effectively processes up to thousands of input data. The irradiance data were recorded for 1000 sample value starting from minimum irradiance of 0 W/m^2 up to maximum irradiance of 1000 W/m^2 . Similarly, for temperature 1000 sample data were recorded starting from minimum temperature of 15°C up to maximum temperature of 35°C. For this two-input data and rating values of the PV module, the feedforward neural network is trained by the formula shown from (14) - (16) with 70% of 1000 sample data utilized for training and 30% for testing and validation. The network is subsequently applied to track V_{MPP} under varying irradiance and temperature conditions, and the resulting deviation from PV voltage is leveraged as a duty cycle. The neural network's tracking performance is best when trained well, as demonstrated in fig. 10.

$$(14) \quad I_{MPP}(i) = I_{mp} * \frac{G}{G_s} + (I + \alpha * (T - T_s))$$

$$(15) \quad V_{MPP}(i) = V_{mp} + \beta * (T - T_s)$$

$$(16) \quad P_{MPP}(i) = V_{MPP}(i) * I_{MPP}(i)$$

where: $V_{MPP}(i)$, $I_{MPP}(i)$ and $P_{MPP}(i)$ are the voltage, current and power respectively at MPP for each sample. In addition, from the training model, the gradient performance of the neural network is indicated in fig. 11.

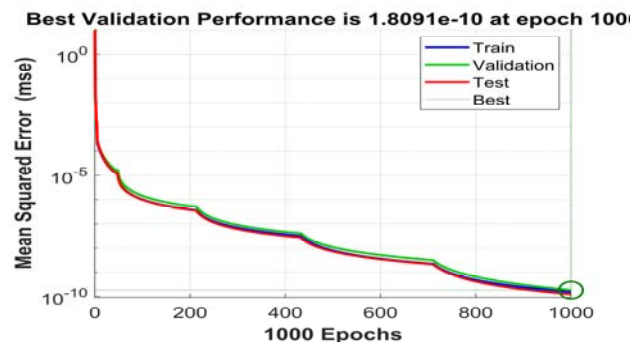


Fig.10. Performance of trained Neural Network

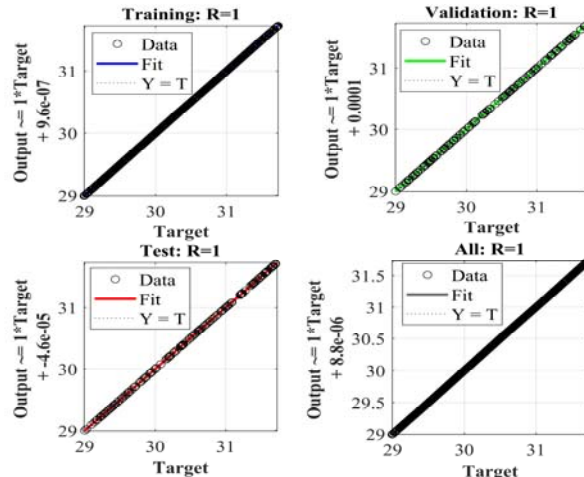


Fig.11. Regression of the trained neural network

ANFIS training, test, and performance evaluation

ANFIS can model nonlinear functions, identify nonlinear components online, and predict chaotic time series in control systems through simulations. Like ANN, ANFIS also trained using two input data (temperature and irradiance) and one output data (V_{MPP}). However, ANFIS can learn from both numeric and linguistic representations.

As indicated in fig. 12, the ANFIS structure consists of two inputs, five membership functions for each input, a rule base based on Takagi-Sugeno fuzzy inference, an output membership function, and the output (V_{MPP}). The ANFIS is trained with Minimal training root mean square error (RMSE) of 9.71166e-07, which indicates a best performance of the trained ANFIS model.

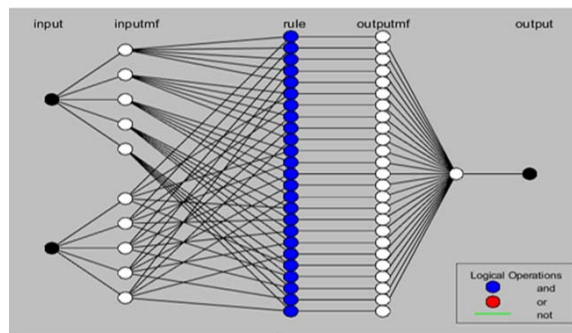


Fig.12. Trained ANFIS structure

Result and analysis

For the proposed methods of ANN and ANFIS, the simulation results are presented for three conditions regarding to the irradiance and temperature variation. Condition 1, simulation result where irradiance and temperature are constant (1kW/m2 and 25°C).

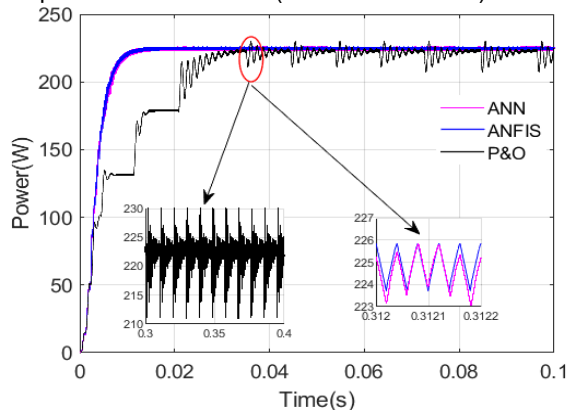


Fig.13. Simulation result of tracked maximum power under constant irradiance and temperature

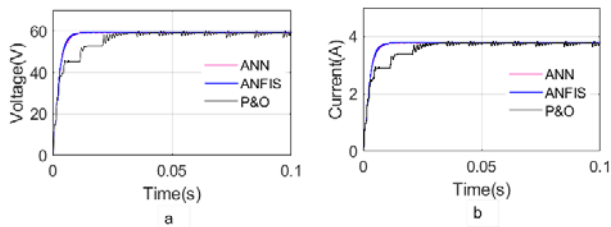


Fig. 14. Simulation result under constant irradiance and temperature (a) Voltage, and (b) Current

Based on the simulation result presented in fig. 13, it can be inferred that the ANN and ANFIS based MPPT algorithms exhibit superior accuracy, efficiency, and tracking response time compared to P&O algorithm for a 230 Wp PV system operating under constant irradiance and temperature conditions. To further quantify the efficiency of the different MPPT algorithms, the maximum steady state power (P_{max}), minimum steady state power (P_{min}), and rated PV system power (P_{rated}) can be calculated and tabulated as shown in table 3.

Table 3. Efficiency calculation for the proposed algorithms

MPPT algorithm	P_{max} (W)	P_{min} (W)	P_{rated} (W)	Efficiency (%)	Response time (ms)
P&O	230	211	230	95.86%	37
ANN	225.8	223	230	97.57%	11
ANFIS	225.8	223.8	230	97.76%	11

The efficiency is calculated as the ratio of the average of the maximum and minimum steady state power to rated PV system power, multiplied by one hundred. table 3., shows that both the ANN and ANFIS-based MPPT algorithms have efficiencies close to 98%, indicating that they can track the maximum power point of the PV system with minimal power losses. The P&O algorithm, on the other hand, has a lower efficiency of 96%, indicating that it is less effective at tracking the maximum power point compared to the ANN and ANFIS algorithms.

Apart from constant irradiance and temperature, the performance of the proposed MPPT algorithm was also evaluated through simulations at different levels of irradiance and temperature, as depicted in fig. 15 and fig. 16. The MPPT algorithm's ability to recover from changes in irradiance levels was tested by subjecting it to variable irradiance levels ranging from 200 W/m^2 to 1000 W/m^2 , followed by 1000 W/m^2 to 200 W/m^2 . The MPPT tracking and recovery performance is illustrated in fig. 15 a & b. The results indicate that ANN and ANFIS MPPT techniques outperform P&O algorithm, especially when there are sudden changes in irradiance levels.

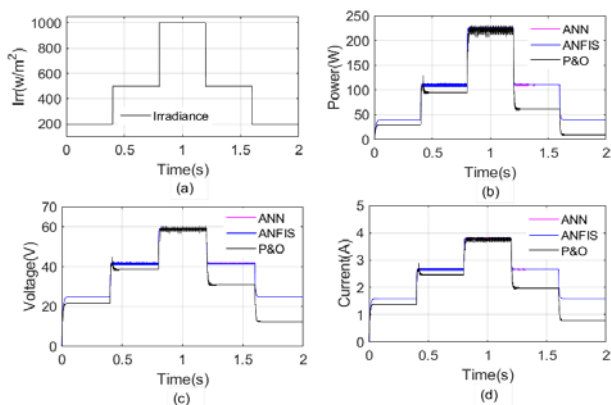


Fig.15. Simulation result under variable irradiance and constant temperature (a) Irradiance, (b) tracked power, (c) tracked voltage, and (d) tracked current

Moreover, the MPPT algorithm's performance was also tested at varying temperatures ranging from 15°C to 35°C, with rapid temperature changes from 35°C to 15°C, as shown in fig. 16 a & b. The results demonstrate that ANN and ANFIS algorithms can effectively track and recover from sudden temperature changes, whereas the P&O algorithm shows poor performance, especially at low temperatures (15°C), it tracks half of the power which is tracked by ANN and ANFIS. In general, the overall comparison of the proposed MPPT algorithm under different factors is indicated in table 4.

Table 4. Comparison among ANN, ANFIS and P&O

Index	ANN	ANFIS	P & O
Tracking efficiency	High	High	Low
Response time	Fast	Fast	Slow
Steady-state oscillation	Low	Low	High
Oscillation around MPP	No	No	Yes
Accuracy	High	High	Low
Adaptability	High	High	Low
Training time	Long	Medium	N/A
Complexity	High	Medium	Low
Robustness	High	High	Low
cost	High	Medium	Low

Condition 2, simulation result where irradiance varies from 200 W/m^2 to 1000 W/m^2 and constant temperature (25°C). Condition 3, simulation result where temperature varies from 15°C to 35°C and constant irradiance (1kW/m²)

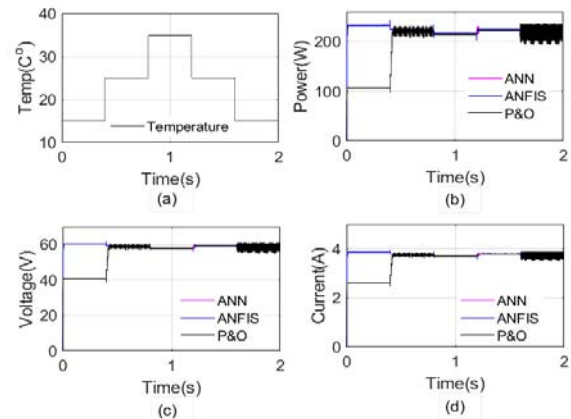


Fig.16. Simulation result under variable temperature and irradiance (a) Temperature, (b) tracked power, (c) tracked voltage, and (d) tracked current

Conclusion

The MPPT performance of the proposed ANN & ANFIS MPPT techniques was evaluated from simulation results under different scenarios, including constant irradiance and temperature, rapid changes in irradiance while temperature remains constant, and rapid changes in temperature while irradiance is constant. The results demonstrated that both techniques exhibited superior tracking efficiency, fast response times, and almost no oscillations around the MPP. They were also found to be highly adaptable to rapid changes in irradiance and temperature, effectively tracking the MPP without any failures, which is a common issue with the P&O MPPT algorithm.

Furthermore, the ANN-based MPPT technique was found to have high accuracy and fast convergence, making it well-suited for real-time applications. However, it requires

a substantial amount of data for training, which can be time-consuming and computationally intensive. On the other hand, the ANFIS-based MPPT technique combines the strengths of neural networks and fuzzy logic systems, providing good accuracy and fast convergence while also being able to handle uncertainties and vagueness. Compared to ANN, ANFIS requires moderate training time and has moderate computational complexity.

Lastly, the P&O-based MPPT technique is simple and easy to implement, making it cost-effective with low computational complexity. However, it has limitations in handling rapid changes in irradiance or temperature, resulting in oscillations around the MPP.

In summary, selecting the appropriate MPPT technique depends on the specific application and requirements. A combination of techniques may also be employed to achieve optimal results. Overall, these techniques play a crucial role in improving the efficiency and performance of PV systems.

REFERENCES

- [1] S. A. Kalogirou, Chapter nine – photovoltaic systems., Second Edition ed., S. E. Engineering, Ed., Academic Press; 2009. p. 469–519., 2014, pp. 481-540.
- [2] K. Sauer, T. Roessler and C. & Hansen, "Modeling the Irradiance and Temperature Dependence of Photovoltaic Modules in PVsyst," *EEE Journal of Photovoltaics*, , vol. 5, pp. 152-158, 2015.
- [3] K. Lapalainen and Valkealahti, "Effects of irradiance transition characteristics on the mismatch losses of different electrical PV array configurations," 2017.
- [4] Tahar, B., Djillali, M., & Khaled, H. (2021). Maximum Power Point Tracking under simplified sliding mode control based DC-DC boost converters. *Przeegląd Elektrotechniczny*, 97(7).
- [5] Y.-H. Liu, C.-L. Liu, J.-W. Huang and J.-H. Chen, "Neural-network-based maximum power point tracking methods for photovoltaic systems operating under fast changing environments," *Solar Energy*, vol. 89, pp. 42-53, March 2013.
- [6] A. Dounis, P. Kofinas, G. Papadakis and C. & Alafodimos, "A direct adaptive neural control for maximum power point tracking of photovoltaic system," *Solar Energy*, 115, 145-165., 2015.
- [7] W. Lin, C. Hong and C. Chen, "Neural-Network-Based MPPT Control of a Stand-Alone Hybrid Power Generation System," *IEEE Transactions on Power Electronics*, 26, 3571-3581., 2011.
- [8] Kumar, Karri Hemanth, and Gadi Venkata Siva Krishna Rao. "A photovoltaic system maximum power point tracking by using artificial neural network." *Przeegląd Elektrotechniczny*, R. 98 NR 2/2022, 98 (2022). doi:10.15199/48.2022.02.07
- [9] Szabat, Krzysztof, et al. "A fuzzy unscented Kalman filter in the adaptive control system of a drive system with a flexible joint." *Energies* 13.8 (2020): 2056.
- [10] Bejmert, D., and W. Rebizant. "Wykorzystanie teorii zbiorów rozmytych do stabilizacji zabezpieczenia różnicowego transformatora." *Przeegląd Elektrotechniczny* 86.8 (2010): 11-15.
- [11] SURYOATMOJO, Heri, Mochamad Ashari, and Nurvita ARUMSARI. "Design and Implementation of MPPT Fuzzy Logic Controller for Inverter Connected to Water Pump." *Przeegląd Elektrotechniczny*, R. 98 NR 8/2022 (2022). doi:10.15199/48.2022.08.27
- [12] M. N. Ali, K. Mahmoud, M. Lehtonen and M. M. F. Darwish, "An Efficient Fuzzy-Logic Based Variable-Step Incremental Conductance MPPT Method for Grid-Connected PV Systems," in *IEEE Access*, vol. 9, pp. 26420-26430, 2021, doi: 10.1109/ACCESS.2021.3058052
- [13] M. Dehghani, M. Taghipour, G. B. Gharehpetian and M. Abedi, "Optimized Fuzzy Controller for MPPT of Grid-connected PV Systems in Rapidly Changing Atmospheric Conditions," in *Journal of Modern Power Systems and Clean Energy*, vol. 9, no. 2, pp. 376-383, March 2021, doi: 10.35833/MPCE.2019.000086
- [14] I. Houssamo, F. Locment and M. Sechilariu, "Experimental analysis of impact of MPPT methods on energy efficiency for photovoltaic power systems," *International Journal of Electrical Power & Energy Systems*, vol. 46, 2013.
- [15] J. SahooSusovon, SamantaSusovon and S. Bhattacharyya, "Adaptive PID Controller with P&O MPPT Algorithm for Photovoltaic System," *IETE Journal of Research* 66(5):1-12, 2018.
- [16] F. M and González-Longatt, "Model of Photovoltaic Module in Matlab™," in *2do congreso beroameri cano de estudiantes de ingeniería eléctrica, electrónica y computación* pp.1-5, 2005.
- [17] T. Salmi, M. Bouzguenda, A. Gastli and A. & Masmoudi, "Matlab/simulink based modeling of photovoltaic cell", *International journal of renewable energy research*, 2(2), 213-218., 2012.